Ahmad Basshofi Habieb

A dissertation submitted in partial fulfillment
of the requirements for the degree of
Doctor of Philosophy
of
University College London.

University College London

Abstract

In developing countries, masonry is generally employed in the construction of residential buildings due to its relatively cheap cost. However, these structures are often provided with inadequate seismic protection. A low-cost base isolation aimed at decreasing the seismic vulnerability of masonry buildings is studied in this work from a numerical standpoint. The studied isolator is an unbonded fiber-reinforced elastomeric isolator (UFREI). With fewer rubber pads than conventional isolators, the proposed UFREI is a cheaper option. A 3D finite element (FE) analysis is performed to predict the behavior of the UFREI under large displacements, capturing the softening and hardening event of the isolator.

The isolation system is then implemented into a two-story masonry building prototype, where the 3D model of a single UFREI is substituted by a nonlinear spring and a damper. A full-scale time-history analysis is performed to evaluate the performance of the isolation system applied in a high-seismic region. During simulation, the inter-story drift and tensile damage of the masonry element are monitored. The results show a promising performance of the proposed isolation with favorable base displacement.

In the other section, a newly Abaqus user-element (UEL) is introduced to predict all 3D behaviors of the UFREIs, based on macroscale computation. The UEL consists of two nodes and 12 degrees of freedom, connecting the foundation to the upper structure. The validation of the UEL is performed through a detailed 3D FE simulation on an isolated rigid slab, employing four different isolators to generate torsion and rotation during seismic motion. Finally, the representative UEL decreases significantly the computational costs of the analysis with an excellent accuracy, compared to the detailed 3D model.

In the end, an experimental study on recycled rubber materials is discussed. The recycled rubber is considered here as a main substance of the UFREIs, to reduce the fabrication cost. The experiment consists of tensile test and relaxation test to characterize the hyperelastic and damping behavior of the recycled rubber. Furthermore, mechanical properties of the rubber are estimated for numerical modeling purpose.

0.1 Introduction

Seismic isolation is an effective solution to reduce the vulnerability of new and existing structures. Isolation can mitigate the negative impact of an earthquake because it shifts the period of the structure in the range of the spectrum where the spectral acceleration is low. Seismic isolators are especially needed for masonry structures in developing countries. Masonry is a common building method in developing countries because of its low cost and simplicity of construction, but its poor tensile strength ultimately leads to low horizontal loading capacities [24, 15]. In high seismicity regions such as Indonesia, many affordable housing structures are built with masonry and experience severe damage during an earthquake. This consequently results in many avoidable casualties [3]. The importance of conceiving new low-cost seismic isolation systems is therefore paramount.

An elastomeric isolator is a well-known and relatively cheap seismic isolation device. Typically, it consists of several layers of high-damping rubber (pads) and reinforced by steel lamina interposed between pads. The reinforcement has the role of limiting only vertical deformations. The horizontal deformations can be large and are controlled by the small shear stiffness of the pads. This system can isolate the energy transmission of the earthquake from the foundation to the upper-structure. However, a massive application of commercial elastomeric isolators in developing regions is not easy to be realized. It still costs too much for its widespread utilization in low-class housing, due to the need of using steel reinforcements and rigid steel plates for isolation supports.

Glass or carbon fiber lamina is now being used as an alternative reinforcement [14, 12]. A glass fiber is much cheaper than its steel counterpart but has a comparable reinforcement effect. Furthermore, one may think to remove the stiff still plates connecting the isolator to ground and superstructure, so conceiving a so called unbonded device , also known as Unbonded Fiber Reinforced Elastomeric Isolator (UFREI). Experimental works reveal the advantages of the UFREI application [33, 30].Its effective horizontal stiffness is considerably lower than that of a bonded device, decreasing the seismic force demands. This softening effect is notable in the stiffness variation of UFREIs that is caused by a roll-over deformation of the UFREI (Fig. 2), which is a sort of quasi rigid rotation occurring at large deformation under strong earthquakes.

Another remarkable feature of a UFREI is the so called hardening at large deformation. This occurs when the vertical edges of the bearing, due to increased roll-over, touch the superstructure and the ground. It is considered as an advantageous effect because it plays an important role in limiting the shear displacement during a maximum seismic motion [37]. An innovative method was proposed to accelerate the full-contact mechanism of a UFREI by modifying the geometry of the upper and bottom supports [37]. However, this method seems to significantly increase the construction cost. The hardening feature is also found in an expensive isolation system that employs a stopper device to control the displacement [7, 39].

UFREIs have been already applied for seismic isolation of low-rise masonry prototypes tested in the laboratory [12]. The experimental results show a desired behavior of the isolated structure with a significant reduction of the roof acceleration and inter-story drift. This excellent performance is also followed by an easy technical detail of the connection between the isolators and the structures. Consequently, advanced and complicated construction methods can be avoided. Basing on such promising results, a first full-scale masonry building isolated with UFREIs has been recently built in Tawang, India, a well know high seismicity region [31].

UFREI specimens in the literature [33, 5, 38] mostly consist of many thin rubber pads (15-20 pads), resulting in high shape factors, defined as known as the ratio between the load area to the force-free area of a single pad. Employing many thin pads, consequently, increases the price because of the need for adhesive on rubber-fiber interfaces. Thus, in this work, a UFREI with significantly fewer rubber pads is proposed to result in a cheaper isolation system.

0.2 Effective numerical modeling of unbonded rubber isolation for masonry housing

Another important issue is the modelling of UFREIs in structural analysis. The non-linearity model of this isolator, including the softening and hardening, is not found in the most structural analyses software available [29, 10]. Some works implemented a numerical model of UFREIs only up to the softening mode [11, 19]. The hardening branch was usually excluded because it was considered as the unstable part.

First of all, a detailed 3D model of a single isolator is implemented into ABAQUS and its hysteretic behavior is numerically analyzed. A preliminary validation is provided assuming as reference some existing experimental data obtained on a standard UFREI subjected to hysteretic cycles. The proposed UFREI is then identified with a single DOF system constituted by a spring exhibiting softening during a cycle, this latter is quite low and can be disregarded without meaningful errors for structural applications. The identification of the 3D model behavior with a single DOF system (non-linear spring with damping) is mandatory to perform large scale non-linear dynamic analyses on isolated full scale buildings.

0.2.1 A numerical model of fiber reinforced elastomeric isolator (FREI)

Fig. 1 shows the isolators considered in the present work. UFREI-200 is the reference specimen [34] to calibrate the material properties, and UFREI-175 is the proposed device with a much fewer number of pads. The isolator is used in unbonded type (UFREI), where the upper and lower edges do not exhibit any bond with the supports. Under moderate shear forces, such frictional limited strength allows the isolator to roll-over and facilitates larger deformations, see fig 2. Unlike a bonded model, the peak tensile stress on the rubbers and interfaces significantly decreases. Thus, delamination at high deformation can be avoided.

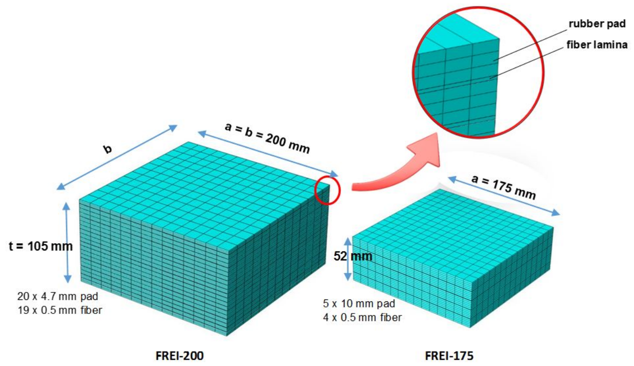

Figure 1: Geometry comparison of isolator UFREI-200 and UFREI-175 and mesh used for the 3D FE analyses

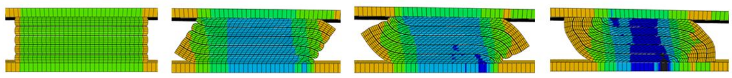

Figure 2: Lateral deformation modes of UFREI

To realistically reproduce experimental results, a hysteresis behavior of the isolator is required. Two of the authors of this research proposed a simplified hysteresis behavior of rubber to be used in FE model by mixing elastoplastic concepts and hyperelastic properties [21]. In the present paper, a similar procedure is adopted. First, we generate a nonlinear behavior through a 3D FE simulation, based only on the hyperelasticity of the rubber pad, i.e., without different loading-unloading paths, see Figure 3b. The dashed line represents the shear behavior obtained by the FE analysis of a UFREI-200. This displacement-force data is then inputted as the properties of a nonlinear spring at a structural level.

Secondly, to generate a hysteresis behavior, a damping coefficient is applied to the spring so that the model can fit the experimental data. In the experiment [33], the equivalent damping of the unbonded FREI-200 was reported to be equal to 5.2%.

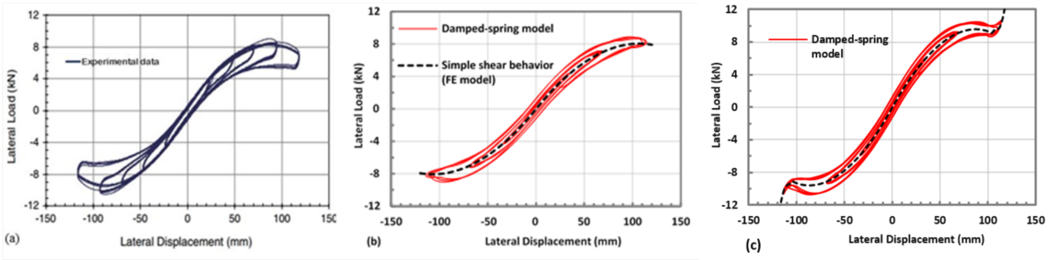

Figure 3: (a) Experimental shear behavior of FREI-200 and shear behavior obtained from 3D-FE model and equivalent damped-spring model of (b) UFREI-200, and (c) UFREI-175

The spring model with damping (fig. 3b) shows a reasonable fitting with the experiment (fig. 2a). However, it cannot catch up the sudden increase of damping as seen in the last cycle of the experiment. Nevertheless, it is noted that this limitation does not affect the final results. With the same procedure, a spring model of UFREI-175 is obtained (fig. 3c). The nonlinear spring model of UFREI-175 is implemented later at the structural level of a two-story isolated masonry building.

0.2.2 Seismic performance of an isolated masonry housing using UFREIs

An FE model of a medium size two-story masonry house with openings and concrete diaphragms at foundation and roof levels is implemented in ABAQUS commercial code. The masonry building taken as reference is an existing one and was constructed in Tawang, India [31] to test the behavior of masonry houses isolated with UFREIs. According to authors' knowledge, this is probably one of the first examples of masonry housing isolation by means of low cost devices. Dimensions of the building are the following: thickness of the walls 300 mm, each room has 4 x 4 m plan dimensions, height of each floor is 3m, see Fig. 4. To prevent premature damage of the walls, rigid beams on top of windows and doors are inserted, in agreement with the real prototype. The numerical model has thinner walls and significantly smaller isolators compared to the real one built in India [31].

In the FE model, masonry is considered as an isotropic material exhibiting

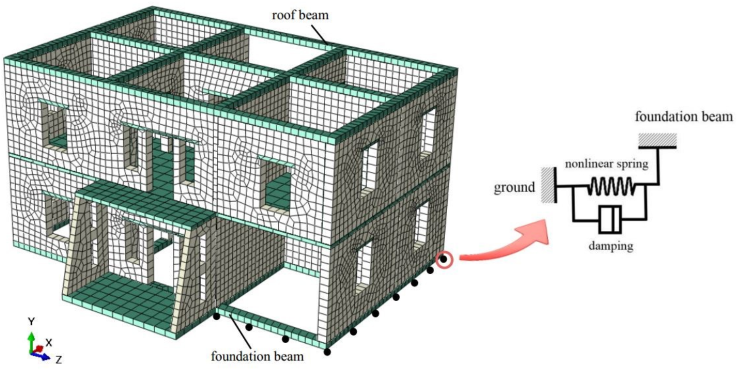

Figure 4: Mesh used for the masonry prototype with isolation system and numerical model adopted at a structural level for a single isolator

damage in both tension and compression. Although it is a simplification, this assumption is commonly accepted in engineering practice [32, 22, 8]. As far as the non-linear behavior is considered, a concrete damage plasticity model (CDP) is adopted. Although CDP is originally conceived for isotropic fragile materials (typically concrete) [36, 6, 1], it can be adapted to masonry because the orthotropy ratio in brickworks is moderate (around 1.2) under biaxial stress states in the compression–compression region [26, 20]. The tensile and compression strengths of the masonry are considered 0.15 and 1.5 MPa, respectively [9].

Fig. 5 presents the damage propagation of the masonry prototype undergoing an accelerogram, without and with isolation. Through a 3D nonlinear time-history analysis, it can be affirmed that the isolated masonry is safe in terms of inter-story drift. The isolated structure is subjected to seven accelerograms according to Indonesian code, with the target location is Timika city, Papua island (0.6g of PGA). The FE model allows the application of two horizontal components of the earthquakes. A moderate damage is present, but only 0.28% as the average of maximum drifts, an outcome which assures the suitability of a low cost isolation. Also, the isolator deformation satisfies the limit of critical deformation. The average value obtained (111 mm) is smaller than the critical shear deformation, which is 300% of total rubber thickness (or 150 mm). This critical value is found through experimen-

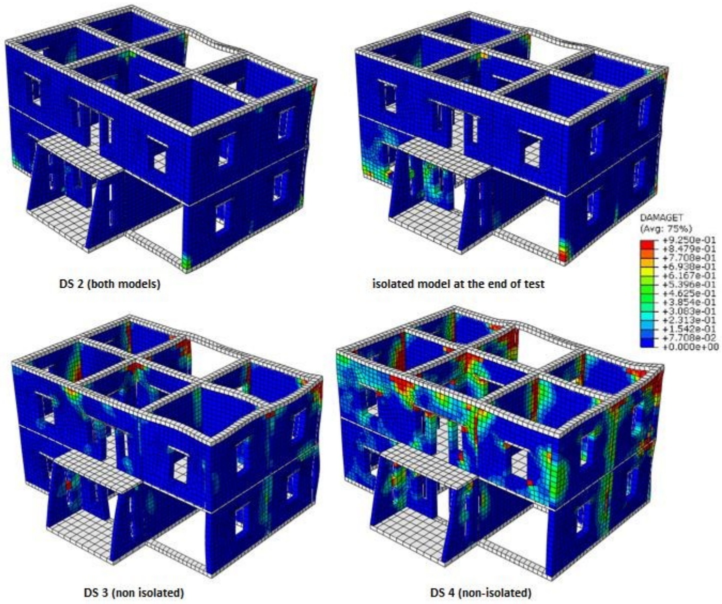

Figure 5: Tensile damage distribution on masonry structures undergoing Chi-chi accelerogram without and without isolation

tal researches [14][13]. It indicates that the isolation system is capable of surviving the selected ground motions.

0.3 An Abaqus user-element for 3D behavior of unbonded fiber reinforced elastomeric isolators (UFREIs) based on macroscale computation

As a matter of fact, the utilization of detailed 3D discretization for UFREIs is computationally expensive, with results not easily achievable for macro-scale computations in the non-linear dynamic range. Therefore, a simple and representative model is paramount. Some works where a simplified numerical model of the horizontal behavior of UFREIs have been recently presented [18, 25, 16], but the behavior in compression, rotation, and torsions are still important parameters not taken sufficiently into account. This section presents a comprehensive but enough simple model for a UFREI which has been implemented in Abaqus as new user element

(UEL) and takes into account the most important features exhibited by such device, such as the softening and hardening effects. This UEL is very useful for full 3D nonlinear dynamic analyses of complex isolated structures to be performed in an advanced FE code (such as Abaqus), which allows taking into account material and geometric nonlinearity.

0.3.1 Analytical solution for 3D behavior of UFREI

In order to calibrate the mechanical properties of the proposed UEL element, a 3D FE model of a U-FREI is previously built by applying hyper-elastic and viscous behaviors for the rubber material. The geometry is presented in Figure 1. The hyperelasticity follows Yeoh strain-energy model, which corresponds to a rubber with shear modulus 0.6 MPa. While the viscous damping, that is characterized by a Prony-series, represents a rubber with 8% of damping.

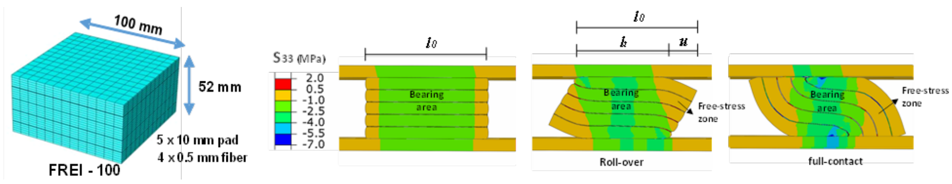

Figure 6: Geometry and shear deformation modes of UFREI-100 under constant vertical pressure

Without bonding on the upper and bottom surfaces, the U-FREI bearing is then subjected to a cyclic horizontal displacement with 0.5 Hz of frequency and a constant vertical pressure 1.17 MPa. The result of FE simulation is presented in Fig. 6 and 7a, showing a remarkable softening of the horizontal stiffness due to rolling-over deformation. In Fig. 6, a free-stress zone appears as the result of the rolling-over. A softening is also captured on the compressive behavior of the U-FREI, see Fig. 7b, with increasing lateral displacement. In Fig. 7b, only one cycle (up to 60mm) is presented to simplify the analysis of the vertical behavior.

$$Ar = b \cdot lt \ (1); \qquad lt = l_0 - (u \cdot ml) \quad (2); \qquad k_H = G.Ar \cdot \frac{\left(1 - \frac{Pl}{Pcr}\right)^2}{h_{rubber}} \quad (3)$$

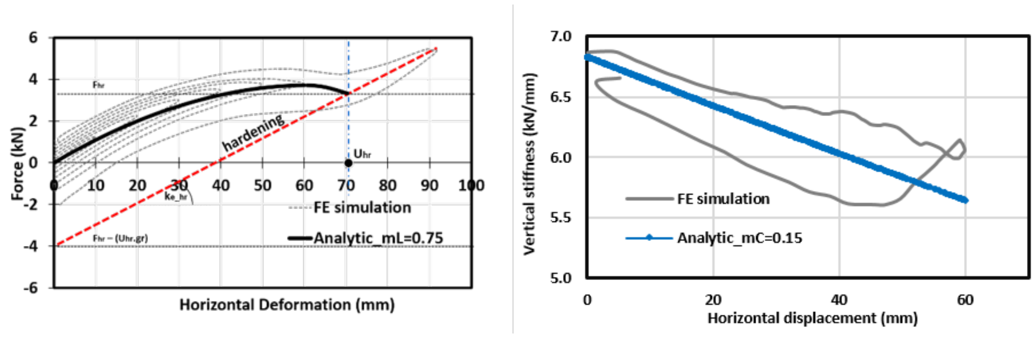

Figure 7: FEA results and analytic solutions of (a) shear behavior and (b) vertical stiffness of UFREI-100

To sum up, the softening is affected by the combined action of the vertical load (*Pl*) and the horizontal deformation (u). Therefore, a suitable variable is introduced into the classic horizontal stiffness equation to generate the softening effect. The governing equation is briefly discussed in this report. In equation 1-3, b is the length of the isolator (perpendicular to the figure), l_0 and l_t are the initial and current length of rubber in shear direction (see Fig.6). The shear stiffness k_H depends on the bearing area *Ar,* which varies due to the shear displacement *u,* while *ml* is a modifying factor to determine the contribution of the free-stress zone. Consistently, a similar method is applied for the vertical stiffness evaluation (see Fig.2b). The fictitious hardening line is generated by estimating the magnitude of shear displacement when the full-contact mode takes place. At this stage, the stiffness is multiplied by a hardening factor. The rotational and torsional stiffness of the UFREI is adjusted by introducing a reduction factor. A study recently presented shows that the rotational stiffness of UFREIs is 25% lower than that of bonded isolators [2]. Meanwhile, through a 3D FE simulation, we did not find any difference in torsional stiffness between bonded and unbonded type, under 1 MPa of vertical pre-loading. In the present model, the rotational and torsional stiffness are considered constant, as they do not affect the global behavior of an isolated structure significantly.

The modified equations are then implemented into a UEL beam element with two nodes (each node has 6 DOFs), connecting the structure to the ground, as seen in Fig 8. To produce a hysteresis behavior, a Bouc-Wen model is implemented in the UEL code, taking into account a coupling mechanism between damping force in x and y direction, as proposed in [17]. The hysteretic behavior of the beam is then evaluated by means of a standard Newton-Raphson procedure. The UEL is implemented as Fortran Abaqus subroutine.

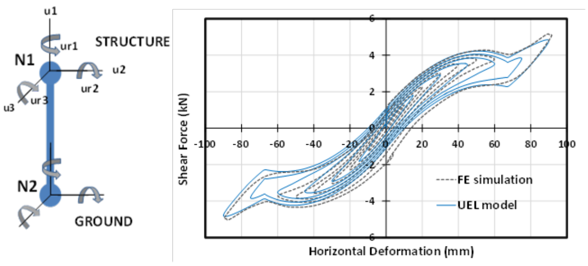

Figure 8: A representative user-element with 12 DOFs and comparative results between UEL and 3D FE modeling on shear behavior of UFREI-100 with hardening

0.3.2 Validation of the UEL in a 3D dynamic analysis

For validation purpose, a dynamic 3D analysis on a simple isolated slab is presented. Four UFREIs are used to seismically isolate the square-rigid slab, as seen in Fig. 9. To generate 3D behaviors of the system including torsion and rotation during seismic excitation, four UFREIs with significant different stiffness are used in the isolation system. Two models are presented in this section. The reference model employs detailed 3D UFREIs with refined mesh and the second uses the proposed UEL as replacement of each UFREI. The isolated system is then subjected to an accelerogram, which is estimated resulting in a moderate displacement of the base isolators. Finally, the UEL model gives an excellent prediction of the detailed 3D FE model, as shown in the comparative results of top acceleration (fig. 10).

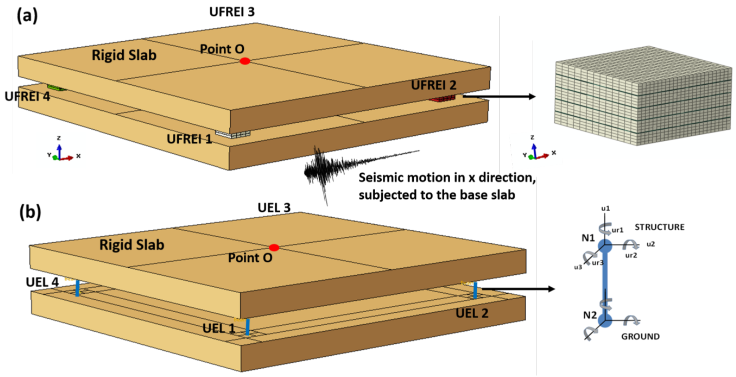

Figure 9: An isolated slab system using (a) 3D FE model, and (b) UEL model

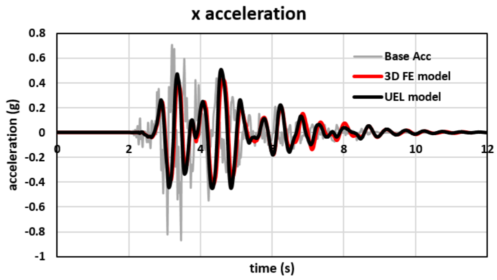

Figure 10: Comparative results of top-slab acceleration between 3D FE model and UEL model

0.4 Experimental study on mechanical characterization of recycled rubber materials

As the present research aims to develop a low-cost rubber isolator, experimental study to observe the behavior of recycled rubbers is performed. The recycled material considered is a deactivated EPDM, produced by DERGOM Srl. In the research field, utilisations of recycled rubber materials for seismic isolation device are found in the literature. [35, 27, 28] investigated granulated rubbers derived from tire waste to be mixed with soil as natural seismic isolation for medium-rise buildings. In case of elastomeric isolators [4, 23], recycled rubber compounds were used to fabricate unbonded fiber reinforced elastomeric isolators (UFREIs), as a cheap isolation system. In this section, a series of experimental works are presented to observe the behavior of recycled rubbers in unaged and aged condition. However, only the unaged specimen is presented in this report, as the aging process is still on-going. This work is essential to evaluate the applicability and durability of the recycled rubber for elastomeric isolation use. The specimens considered are RR-30 and RR-70, in which the recycled material contents are 30% and 70%, respectively.

0.4.1 Uniaxial tensile test

Three unaged specimens in the form of dumb-bell pieces (fig. 11) were tested in the uniaxial tensile test device in Polimi laboratory. The result of the tensile test is presented in fig. 12, where the specimen is stretched up to the limit of failure. As expected, the stiffest tensile curve is presented by the rubber with highest shear modulus, but it exhibits the lowest failure strain.

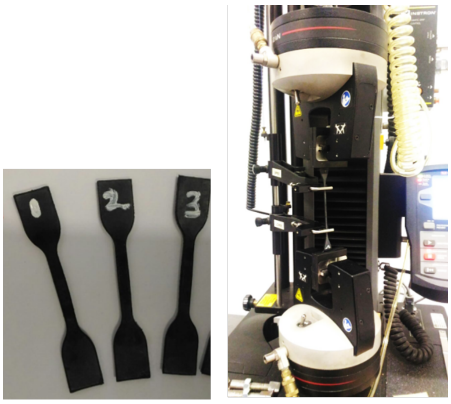

Figure 11: Recycled rubber specimens and the uniaxial tensile device

The hyperelastic parameters obtained are then implemented in the uniaxial tensile test simulation to evaluate the performance of the model. The element used is C3D20R (quadratic) to facilitate excessive deformation. Fig. 13 presents the FE model of the dumb-bell specimens undergoing tensile loading, based on some hyperelastic models. The Ogden model results in the most accurate prediction on the tensile behavior, while the Arruda-Boyce model gives the worst.

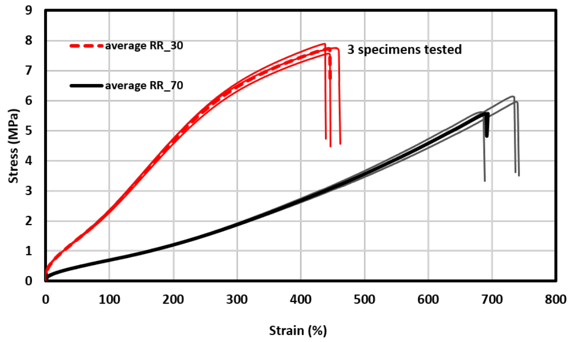

Figure 12: Experimental results of tensile test on specimen RR-30 and RR-70

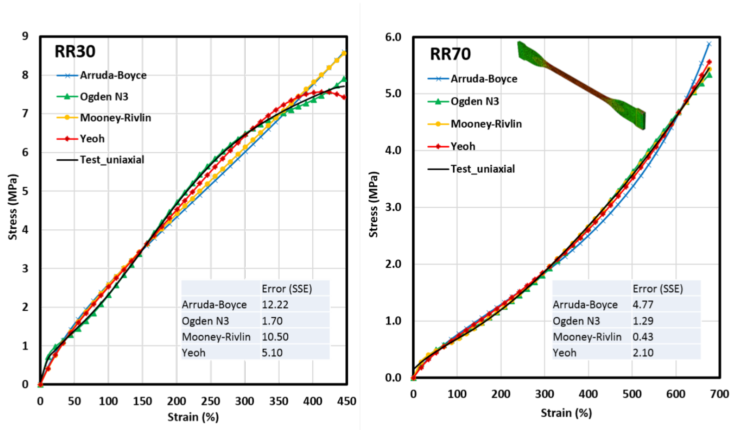

Figure 13: Comparative figure of FE model on the specimens under tensile test

0.4.2 Relaxation test

The relaxation test is meant to obtain viscous properties of the rubber, in this case, based on Prony model. The device for relaxation test is the same as that for the uniaxial test. The first step of the test is to stretch the specimen up to the specified strain, and the device then keeps the strain constant for some period. During that period, the tensile stress is recorded. That stress is gradually decreased in the function of time, while the strain is kept constant. This phenomenon is called as relaxation of the rubber. Having higher damping, the variation between initial and final stress during the constant strain period is greater.

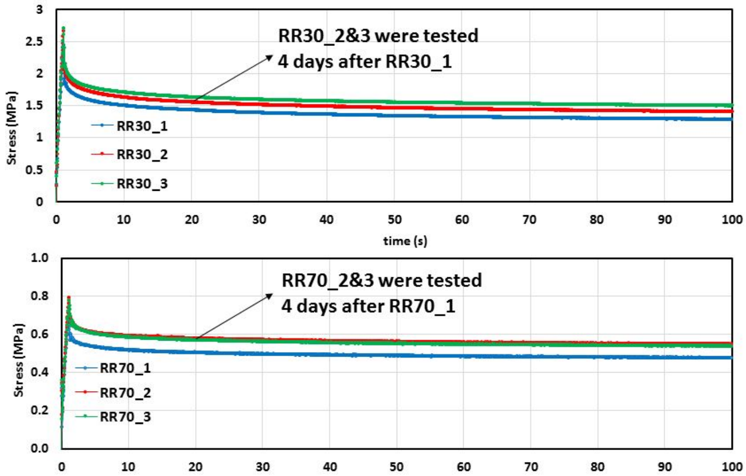

Figure 14: Relaxation test results

The results of relaxation test are presented in fig. 14, showing three tests on each specimen. All specimens are in unaged condition. However, within four days at room temperature, the specimens show a remarkable difference in relaxation behavior. Finally, fig. 15 shows an accurate fitting of Prony series model on both specimens. Having hyperelastic and viscous properties of the specimens, we are able to simulate the rubber behavior in 3D FE analyses.

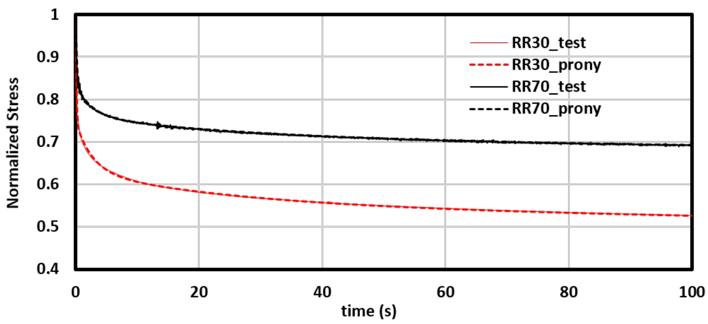

Figure 15: Fitting curve of Prony viscous model

Bibliography

[1] Maurizio Acito, Massimiliano Bocciarelli, Claudio Chesi, and Gabriele Milani. Collapse of the clock tower in Finale Emilia after the May 2012 Emilia Romagna earthquake sequence: Numerical insight. *Engineering Structures*, 72:70–91, 2014.

[2] Yasser M. Al-Anany and Michael J. Tait. A numerical study on the compressive and rotational behavior of fiber reinforced elastomeric isolators (FREI). *Composite Structures*, 133:1249–1266, dec 2015.

[3] Teddy Boen. *Yogya Earthquake 27 May 2006: Structural Damage Report*. EERI, 2006.

[4] Andrea Calabrese, Mariacristina Spizzuoco, Giorgio Serino, Gaetano Della Corte, and Giuseppe Maddaloni. Shaking table investigation of a novel low-cost, base isolation technology using recycled rubber. *Structural Control and Health Monitoring*, 22(1):107–122, apr 2014.

[5] Andrea Calabrese, Mariacristina Spizzuoco, Giorgio Serino, Gaetano Della Corte, and Giuseppe Maddaloni. Shaking table investigation of a novel, low-cost, base isolation technology using recycled rubber. *Structural Control and Health Monitoring*, 22(1):107–122, 2015.

[6] Giovanni Castellazzi, Antonio Maria D?Altri, Stefano de Miranda, and Francesco Ubertini. An innovative numerical modeling strategy for the structural analysis of historical monumental buildings. *Engineering Structures*, 132:229–248, 2017.

[7] Muhammad Tariq Amin Chaudhary, Masato Abé, and Yozo Fujino. Performance evaluation of base-isolated Yama-agé bridge with high damping rubber bearings using recorded seismic data. *Engineering Structures*, 23(8):902–910, 2001.

[8] Thainswemong Choudhury, Gabriele Milani, and Hemant B. Kaushik. Comprehensive numerical approaches for the design and safety assessment of masonry buildings retrofitted with steel bands in developing countries: The case of India. *Construction and Building Materials*, 85:227–246, 2015.

[9] Thainswemong Choudhury, Gabriele Milani, and Hemant B. Kaushik. Comprehensive numerical approaches for the design and safety assessment of masonry buildings retrofitted with steel bands in developing countries: The case of India. *Construction and Building Materials*, 85:227–246, jun 2015.

[10] SAP2000 V CSI. 8, 2002. Integrated Finite Element Analysis and Design of Structures Basic Analysis Reference Manual. *Computers and Structures, Inc., Berkeley, California, USA*, 2010.

[11] Animesh Das, Sajal Kanti Deb, and Anjan Dutta. Comparison of Numerical and Experimental Seismic Responses of FREI-Supported Un-reinforced Brick Masonry Model Building. *Journal of Earthquake Engineering*, 20(8):1239–1262, 2016.

[12] Animesh Das, Sajal Kanti Deb, and Anjan Dutta. Shake table testing of un-reinforced brick masonry building test model isolated by U-FREI. *Earthquake Engineering & Structural Dynamics*, 45(2):253–272, 2016.

[13] Michael GP de Raaf, Michael J Tait, and Hamid Toopchi-Nezhad. Stability of fiber-reinforced elastomeric bearings in an unbonded application. *Journal of Composite materials*, 45(18):1873–1884, 2011.

[14] N. C. Van Engelen, M. J. Tait, and D. Konstantinidis. Horizontal behaviour of stable unbonded fiber reinforced elastomeric isolators (SU-FREIs) with holes.

In *Proceedings of the 15th World Conference on Earthquake Engineering*. Proceedings of the 15th World Conference on Earthquake Engineering, 2012.

[15] Yuan Feng, Dan Yi, and Qiong Bi. Seismic design analysis of the country masonry school buildings in the meizoseismal area. *Earthquake Engineering and Engineering Vibration*, 10:359–367, 2011.

[16] A.B Habieb, G. Milani, T. Tavio, and F. Milani. SEISMIC PERFORMANCE OF A MASONRY BUILDING ISOLATED WITH LOW-COST RUBBER ISOLATORS. In *Earthquake Resistant Engineering Structures XI*. WIT Press, jul 2017.

[17] Manish Kumar, Andrew S. Whittaker, and Michael C. Constantinou. An advanced numerical model of elastomeric seismic isolation bearings. *Earthquake Engineering & Structural Dynamics*, 43(13):1955–1974, apr 2014.

[18] Ali Manzoori and Hamid Toopchi-Nezhad. Application of an Extended Bouc-Wen Model in Seismic Response Prediction of Unbonded Fiber-Reinforced Isolators. *Journal of Earthquake Engineering*, 21(1):87–104, feb 2016.

[19] Ali Manzoori and Hamid Toopchi-Nezhad. Application of an extended Bouc-Wen model in seismic response prediction of unbonded fiber-reinforced isolators. *Journal of Earthquake Engineering*, 21(1):87–104, 2017.

[20] G. Milani, Paulo B. Lourenço, and A. Tralli. Homogenised limit analysis of masonry walls, Part I: Failure surfaces. *Computers & structures*, 84:166–180, 2006.

[21] G. Milani and F. Milani. Stretch–stress behavior of elastomeric seismic isolators with different rubber materials: numerical insight. *Journal of Engineering Mechanics*, 138:416–429, 2011.

[22] Gabriele Milani and Gennj Venturini. Safety Assessment of Four Masonry Churches by a Plate and Shell FE Nonlinear Approach. *Journal of Performance of Constructed Facilities*, 27:27–42, 2011.

[23] Huma Kanta Mishra, Akira Igarashi, and Hiroshi Matsushima. Finite element analysis and experimental verification of the scrap tire rubber pad isolator. *Bulletin of Earthquake Engineering*, 11(2):687–707, oct 2012.

[24] C. V. R. Murtyl, Jayanta Dutta, and Sudhir K. Agrawal. Twin lintel belt in steel for seismic strengthening of brick masonry buildings. *Earthquake Engineering and Engineering Vibration*, 3:215–222, 2004.

[25] Peyman M. Osgooei, Michael J. Tait, and Dimitrios Konstantinidis. Non-iterative computational model for fiber-reinforced elastomeric isolators. *Engineering Structures*, 137:245–255, apr 2017.

[26] A. W. Page. 8487 The biaxial compressive strength of brick masonry. 1981.

[27] Anbazhagan Panjamani, Manohar Devarahalli Ramegowda, and Rohit Divyesh. Low cost damping scheme for low to medium rise buildings using rubber soil mixtures. *Japanese Geotechnical Society Special Publication*, 3(2):24–28, 2015.

[28] K. Pitilakis, S. Karapetrou, and K. Tsagdi. Numerical investigation of the seismic response of RC buildings on soil replaced with rubber–sand mixtures. *Soil Dynamics and Earthquake Engineering*, 79:237–252, dec 2015.

[29] DS Simulia. ABAQUS 6.13 User's manual. *Dassault Systems, Providence, RI*, 2013.

[30] Mariacristina Spizzuoco, Andrea Calabrese, and Giorgio Serino. Innovative low-cost recycled rubber–fiber reinforced isolator: experimental tests and finite element analyses. *Engineering Structures*, 76:99–111, 2014.

[31] Van Ngo Thuyet, SK Deb, and A Dutta. Mitigation of Seismic Vulnerability of Prototype Low-Rise Masonry Building Using U-FREIs. *Journal of Performance of Constructed Facilities*, 32(2):04017136, 2017.

[32] Simone Tiberti, Maurizio Acito, and Gabriele Milani. Comprehensive FE numerical insight into Finale Emilia Castle behavior under 2012 Emilia Romagna seismic sequence: damage causes and seismic vulnerability mitigation hypothesis. *Engineering Structures*, 117:397–421, 2016.

[33] Hamid Toopchi-Nezhad, Michael J Tait, and Robert G Drysdale. Testing and modeling of square carbon fiber-reinforced elastomeric seismic isolators. *Structural Control and Health Monitoring*, 15(6):876–900, 2008.

[34] Hamid Toopchi-Nezhad, Michael J. Tait, and Robert G. Drysdale. Testing and modeling of square carbon fiber-reinforced elastomeric seismic isolators. *Structural Control and Health Monitoring*, 15(6):876–900, oct 2008.

[35] Hing-Ho Tsang, S. H. Lo, X. Xu, and M. Neaz Sheikh. Seismic isolation for low-to-medium-rise buildings using granulated rubber-soil mixtures: numerical study. *Earthquake Engineering & Structural Dynamics*, 41(14):2009–2024, feb 2012.

[36] Marco Valente and Gabriele Milani. Non-linear dynamic and static analyses on eight historical masonry towers in the North-East of Italy. *Engineering Structures*, 114:241–270, 2016.

[37] Niel C Van Engelen, Dimitrios Konstantinidis, and Michael J Tait. Structural and nonstructural performance of a seismically isolated building using stable unbonded fiber-reinforced elastomeric isolators. *Earthquake Engineering & Structural Dynamics*, 45(3):421–439, 2016.

[38] Thuyet Van Ngo, Anjan Dutta, and Sajal K Deb. Evaluation of horizontal stiffness of fibre-reinforced elastomeric isolators. *Earthquake Engineering & Structural Dynamics*, 46(11):1747–1767, 2017.

[39] Krzysztof Wilde, Paolo Gardoni, and Yozo Fujino. Base isolation system with shape memory alloy device for elevated highway bridges. *Engineering structures*, 22(3):222–229, 2000.